Development of Methodology for the Characterization of Toughness in Ductile Fracture

Vítor R. A. Martins

vitor.martins@tecnico.ulisboa.pt

Instituto Superior Técnico, Universidade de Lisboa, Portugal

October 2020

Abstract

This investigation has as goal the development of a test machine and experimental procedure to be used in future studies for the quantification of the mode II fracture toughness of different materials, under different stress states. This new machine allows the use of test pieces, with simple geometry, that can be put under different stress states, which can be set by the test machine.

Keywords: Chip removal machining; Fractur Mechanics; Triaxiality; Test machine;

1. Introduction

The understanding of fracture mechanics is crucial to prevent the failure of the materials that constitute everyday objects that we rely on. Nonetheless the ability to cause these phenomena in a controlled way is as or more important, since fracture is the basis of many production technologies, such as everyone that uses chip removal cutting as the main transformation mechanism. In these technics, controlling the way the cut happens is very important, since these characteristics have an enormous effect in the properties of the final product.

Nowadays the main way engineers use to predict these behaviors is by simulations using FEM. In these simulations a material model must be inserted. These models consist in data, acquired experimentally, that describes the material behavior. One of the characteristics that influences the fracture is the material's fracture toughness. Many factors influence

The goal of this study is to develop a test machine capable of doing the necessary tests for the characterization of the mode II fracture toughness of a material, under different stress states, in a fast and cheap way. To confirm the machine's capabilities an experimental methodology was developed, to verify the machine and to be used in future studies. For these tests a new test piece was developed.

2. Numerical Model

To set the specifications of the test machine regarding force and span simulations were made. These simulations were later used to help in the verifications of the test machine and its results, by comparing the experimental results with the theoretical results. These simulations were made using ABAQUS, a FEM software.

Some steps were taken in verifying that the model reproduced correctly the real material behavior.

2.1 Material Behavior

The first step taken in proving that the material model was correct was proving that the material behaved as expected, during the simulation. For this purpose, a compression test was modeled, that consisted in the compression of a 7mm diameter, 6mm height test piece. This test is the same as the one used by Gregório (2017), which originated the data set used as material law in this model.

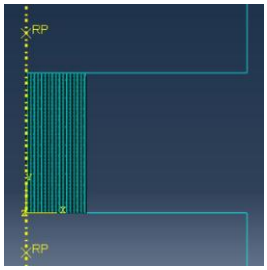

Figure 1- Compression test mesh;

If the simulation model was correct the data at the end of the simulation should be the same as the one obtained by Gregório.

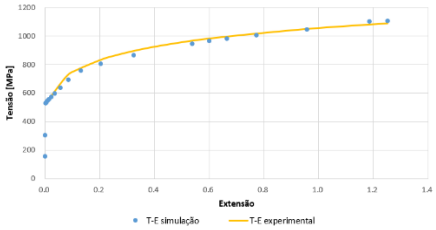

Figure 2- Input (yellow) and output (blue) stress-strain curves;

Figure 2 shows the comparison between the input data, yellow, and the output data, blue. Through the analysis of the figure its confirmed that the model created reproduces well the real material behavior under compression. Although, this model doesn't consider the material fracture behavior, meaning that the material has a pure elastic-plastic behavior. This difference has to be taken into account when estimating the maximum cutting force and when comparing the theoretical and experimental results.

2.2 2D and 3D Comparison

The model used in this study was a 2D model, due to the lack of computational capabilities for the use of a 3D model. The use of a 2D model instead of a 3D one, presents a problem for the accuracy of the simulation. The 2D simulation considers that all the test piece is under plane strain. This isn't true, a small region near the piece surface is under plane stress. The 3D model considers these two regions.

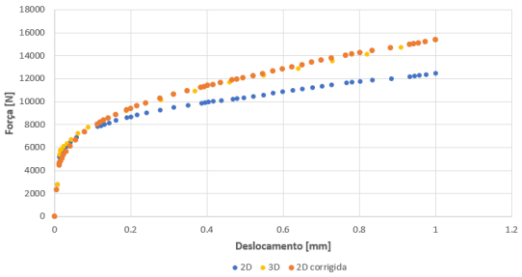

Figure 3- 2D (blue), 3D (orange) and 2D corrected (yellow) force-displacement curves;

Figure 3 shows the comparison of both curves. The difference between both models is very noticeable, so a correction factor was applied to the 2D mode results. This correction factor is shown in equation (1), where $\boldsymbol{F}$ is the force given by the simulation, $\boldsymbol{d}$ is the corresponding displacement and $\boldsymbol{F_c}$ is the corrected force.

$$\boldsymbol{F_c = F * \left(1.23 * d^{1/12}\right)} \qquad \textbf{(1)}$$

The usage of this correcting factor results in the yellow curve in figure 3, that is much closer to the 3D result.

Is important to notice that this correction only applies to this type of experiment and test piece. A slight change, such as increasing the width of the test piece, invalidates this correction factor.

2.3. Sensitivity Analysis

To optimize the usage of computational resources, a sensitivity analysis was made. In it was studied how the element size influenced the maximum cutting force and the calculation time, stopping the mesh refinement when the first stabilizes in one value or when the second gets too big.

As seen before, there are no fracture conditions implemented in this model, resulting in a permanent increase of the cutting force. So, the maximum cutting force is defined has the force at the moment the displacement is equal to the notch height, since the deformation at this point is more than enough to cause the material's failure.

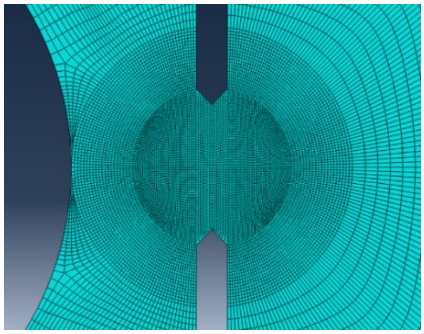

Figure 4- Final mesh;

Early in the analysis it's noticeable that only the elements near the cutting plane, suffer deformation. So, two areas were created in the mesh, a more refined one, near the cutting plane, and another, less refined, in the rest of the test piece, as shown in figure 4.

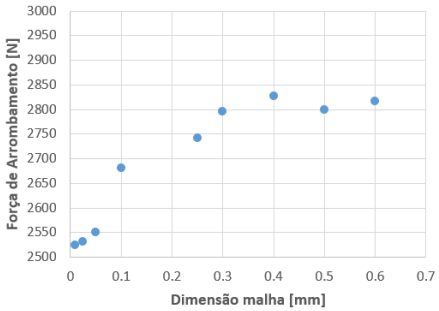

Figure 5- Sensitivity analysis maximum cutting force results;

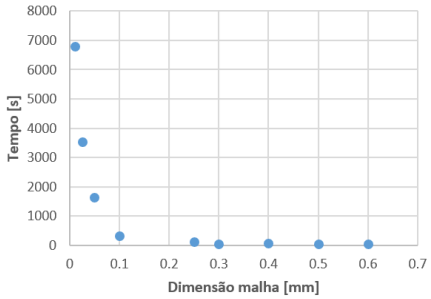

Figure 6- Sensitivity analysis computing time results;

As seen in figure 5, the mesh starts to stabilize for elements with 0,05mm. This is also the point where the computation time starts to increase abruptly. Then, is defined that the optimized mesh, and the one used for the duration of this study, has two zones, one with element size of 0.05, near the cut plane, and the other with 0.2mm, for the rest of the test piece.

3. Test Machine Development

The development of the test machine, done in this study can be divided in three phases: test machine; test tool; data acquisition instrumentation.

3.1. Test Machine

This study requires a machine capable of generating a cutting force and a force normal to the cutting plane. Since there is no machine available that can do both, the responsibility of exerting these forces is divided between the test machine and the test tool. So, there's the need of a machine capable of generating a cutting force of 20kN, as demonstrated in a future chapter, that allows the fracture of the test piece under quasi-static conditions.

For this purpose, a pneumatic press was selected from the laboratory. The selected press is a SCHMIDT pneumatic press, *Steuerung Typ 32* model, that is able to exert 15kN, at maximum pressure, per manufacturer specifications. However, quick test, reveals that the press is only

capable o exerting 11kN at 8bar, 12kN if the pressure is increased to 10 bar.

This force is insufficient for the purposes of this project, so, an alteration was made to the mechanism that multiplies the force of the pneumatic actuator.

The mechanism that allow the increase in force is a knee lever, as shown in figure 7.

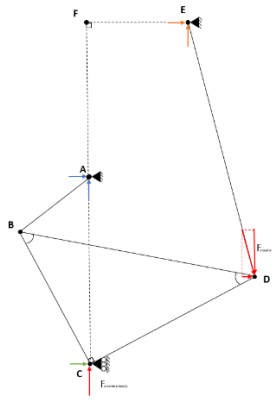

Figure 7- Knee lever force scheme;

A static analysis to the forces was made, arriving at the dimensions presented in table 1. For this analysis was defined that the force required for this study must be exerted at 2mm from the press maximum extension, since the press position influences the maximum force the press can make.

Tabela 1

Braço	$\overline{AB}$	$\overline{BC}$	$\overline{CD}$	$\overline{AF}$	$\overline{EF}$
Dimensão [mm]	20,5	25	110	50	31

To accomplish this change there was the need to produce 3 new components. These components were made in AISI1045 steel, using conventional machining technics.

3.2. Test Tool

The test tool it the tool that will be mounted in the test machine. This tool has to fulfill all the test requirements that the test machine can't. These include transfer the cutting force provided by the press to the test piece, supporting all the data instrumentation and exert the normal force.

To accomplish the first goal a punch and die combo was produced using traditional machining methods and wire cut EDM. This combo was mounted in a support, that guarantees the alignment between the punch and the die, as shown in figure 8.

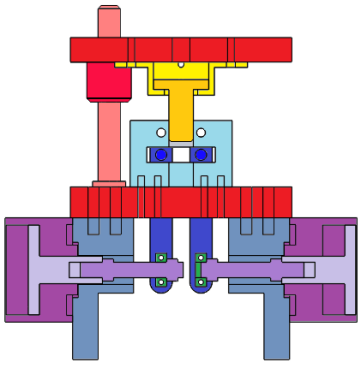

Figure 8- Test machine scheme;

To accomplish the second goal, different ways of support were applied, depending on the type of sensor.

The load cell was mounted in series with the punch, using a housing that allows the free movement of both components when the press is activated and restricted movement when deactivated, as seen in figure 9.

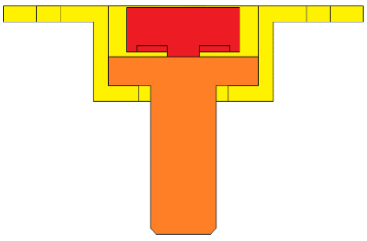

Figure 9- Load cell housing scheme;

The displacement sensor was mounted in the tool support, in parallel with the die punch combo, as shown in figure 10.

Figure 10- Dispacement sensor and camera and respective supports;

For the camera, an adjustable support was developed, allowing easier image capture setting. This mount is also visible in figure 10.

The third goal was accomplished using two pneumatic actuators, that are able to create 3.1kN when extending and 2.8kN, at 10bar, when contracting. This force is insufficient, so a lever system was crated that allow a force multiplication of 6,2 times, resulting in a compression force of 19kN and a traction force of 17kN, at 10bar. Both configurations and all the mechanism are shown in figure 8.

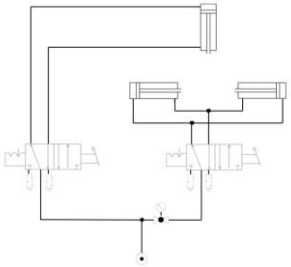

Figure 11- Pneumatic diagram;

To activate both the pneumatic press and the tool pneumatic actuators, the was the need to feed the with pressurized air. For this propose an air compressor was used, with maximum capacity of 10bar, and a pneumatic system was created, schematized in figure 11. This system includes two switches, allowing the independent activation of the tool and press actuators, and a pressure valve in the tool line, that allows the control of the force normal to the cutting plane through the following equations, where F_c is the compressive force and F_t is the traction force:

$$F_c = 19327 * P\ [N] \quad (2)$$

$$F_t = 17379 * P\ [N] \quad (3)$$

3.3. Data acquisition

The characterization of materials fracture toughness, under different stress states, requires three types of data, cutting force value, the value of the force normal to the cutting plane and material displacement. For the collection of these data different technics were implemented.

Additionally, existed the need to record the test piece during the experiment, and to collect all the data for them to be processed.

3.3.1. Cutting Force

For the quantification of the cutting force a DAYSENSOR DYHW-116 load cell was used, as shown in figure 12. This cell consists in an extensometric load cell, with a maximum capacity of 49kN, that requires an excitation current of 10VDC and an amplification of the output signal. These two goals were fulfilled by a Krenel CEL10-A signal amplifier. This amplifier had to be supplied with a 24VDC current, which was supplied by the electric grid through a MEANWELL DR-15-24 font.

Figure 12- Load cell;

This setup went through a calibration process, with known weights, to

guarantee the veracity of the reading, resulting on the calibration equation (4), where F_e is the electric potential that the amplifier outputs and ***F*** is the load applied to the sensor.

$$\boldsymbol{F[N] = 4900 * F_e[V]} \quad \textbf{(4)}$$

3.3.2. Displacement

The displacement was measured using a SONSEIKO KTR-10mm sensor, as seen in figure 13. This is an extensometric sensor, with a 10mm span, that needs a 5V excitation current. This current is provided by a MEANWELL DR-15-5.

Figure 13- Displacement sensor;

This setup also needed to be calibrated. A calibration process, using calibrated shims, resulting in the calibration equation (5), where $d_e$is the electric potential given by the sensor and ***d*** is the displacement.

$$\boldsymbol{d[mm] = 2 * d_e\ [V]} \quad \textbf{(5)}$$

3.3.3. Force Normal to Cutting Plane

Since the force that the lateral actuators remain constant during the duration of the experiment, there is no need to use a sensor, to capture the evolution of this force along the experiment, we only need to know the initial force. To calculate this force, we only need to know the air pressure inside de actuator chamber, and then applying it to equation 3 or 4. This pressure is controlled by a pressure valve coupled to a pressure gauge.

3.3.4. Image Capture

For the recording of the experiment a simple USB Jiansu Atacade camera, with internal lighting, was used. This camera was connected to the computer and the program AMCAP was used to record the video, on a 1080x720 resolution at 5000fpm.

3.3.5. Data Acquisition

To transfer the data given by the sensors to the computer a National Instruments NI-USB6008 DAQ was used. This device allowed the transformation of the analogic data given by the sensors to a digital signal.

This digital data was processed by a virtual laboratory, in LabVIEW, that compiled it and outputted a text file.

4. Methods and Materials

To verify the test machine capabilities a shot experimental study was created. This study was based on an Atkins (2000) study, where he quantified a material's mode II fracture toughness under compressive stress state, with the due changes, to allow the testing under traction stress states too.

This experimental study also has the objective of setting an experimental procedure to be used in future studies.

4.1. Test Piece

The test piece used in this study is a double notched, 8mm thick, rectangular cuboid, to which two holes were added, as represented in figure 14

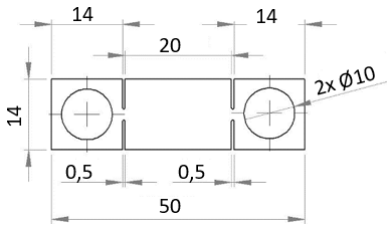

Figure 14- Test piece dimensions;

The test pieces were made from AISI1045 steel, using conventional machining techniques and wire EDM for the notches. Unfortunately, the features made by conventional means were made with low accuracy, resulting in geometrical deviations from the original. These deviations had to be considered in the simulations.

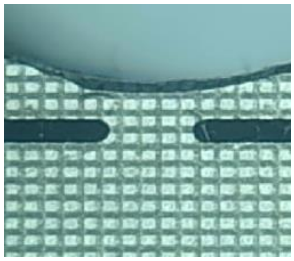

Figure 15- Test piece geometry defect;

4.2 Test Plan

The test plan developed, to verify the machine capabilities, consisted in testing four test pieces under different circumstances.

In the first test a 0,5mm notch thickness test piece was cut, without any force normal to the cutting plane applied. This test, due to how quickly it happened, served to test the test machine capability to capture the test data.

In the second test, a 1mm notch thickness test piece was cut under similar conditions to the previous test. This test proved that the test machine was able of doing the necessary cutting force. In conjunction with the first test, it was used to evaluate what influence the size of the resisting section had over the cutting force.

The third and fourth test also used a 1mm notch test piece. One of the pieces was subjected to a 1,9kN compressive force, normal to the cutting plane, and the other to a 1,7kN traction force. These tests proved the machine's ability to put the test piece under different types of stress states. It also served to evaluate how the stress state influences the cutting force.

4.3. Test Machine Calibration and Verification

Two things need to be verified before the start of the tests, that the test machine can exert the cutting force and that the sensors are working properly in the machine.

Maximum Cutting Force

To verify that the test machine was able to exert the cutting force needed for the test an experimental operating curve was made. This curve was made by registering the cutting force made by the press, at different distances of the upper resting point. During this analysis two problems were detected.

The first problem was the slipping of the press head, which houses al the press mechanisms. This is a problem because the maximum cutting force exerted in the test piece is highly influenced by the press position. To solve this problem a screwed union was added between the press head and the press body, as shown in figure 16.

Figure 16- Press head stop;

The second detected problem was the inversion of the knee mechanism, as shown in figure 17. This phenomenon

happens when the cutting force needed to fracture the test piece is high. The high force exerted by the press causes its structure deformation. This deformation allows the press to pass its lower neutral point, without reaching the high forces predicted by the theoretical operating curve, figure 18.

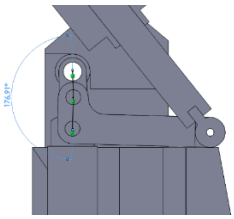

Figure 17- Knee mechanism inversion;

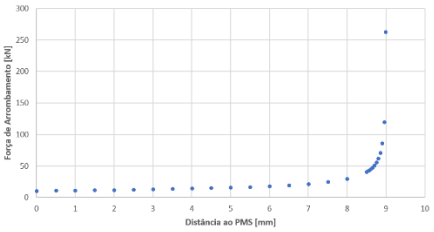

Figure 18- Theoretical press operating curve;

This problem can only be solved by increasing the machine's rigidity. One easy way of doing this change is to add support and close the machine's open C like structure. How ever this would hinder its use and worsen the overall look, and seeing that the current forces are sufficient for the purposes of this study, no further alteration was made, resulting in the final operational curve, figure 19.

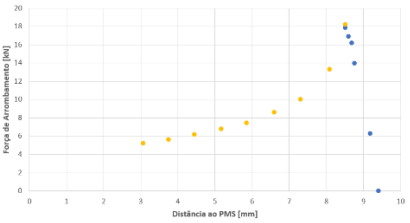

Figure 19- Real press operating curve;

Sensors

The displacement sensor needs no further testing beyond the calibration previously done, just needing to ensure that the sensor is always engaged in the duration of the test and that its mounted vertically and the stop is mounted horizontally, ensuring a true reading.

On the other hand, the load cell required some testing. The first this to test was if the cell housing had any influence it the reading. For this another calibrated load cell was mounted in place of the die. Both cells had the same values, confirming that none of the other components had influence in the load readings. However, during this test a strange behavior was detected, a dampening in the unloading was found, instead of it being instantaneous.

A second test was made to find the origin of this dampening. For this the load cell was mounted in a hydraulic press, as shown in figure 20. This test concluded that this dampening was a property of the load cell/amplifier combo. This claim is supported by the amplifier specifications.

Figure 20- Hydraulic press test;

The sensor calibration had, also, to check if the sensors were synchronized with each other. By testing both sensors simultaneously in the test machine the transitions on both sensors matched, figure 21, concluding that they were synchronized.

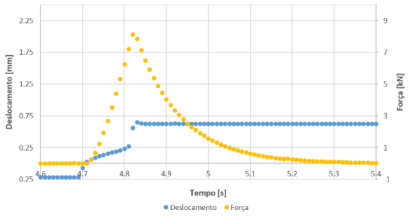

Figure 21- Force and displacement curves;

5. Results and Discussion

As mentioned before, the tests done during this study had two objectives, check if the test machine was able of doing this type of tests, which was the main goal, and a secondary objective, regarding the comparison between the predictions and the reality, and good were those predictions.

The first prediction made was regarding the influence that the resistant area had in the cutting force. Three simulations were made, only varying the notch size, and consequentially the resistant area. The results are shown in figure 22, concluding that the cutting force will increase with the increase in resistant area.

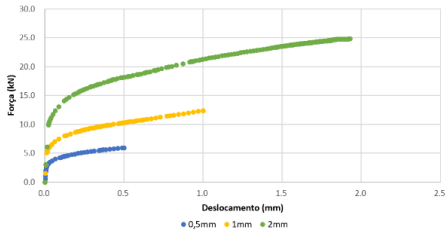

Figure 22- Notch size comparison force-displacement curves;

The second prediction made was regarding the influence that the force normal to the cutting plane had in the cutting force. Two sets of simulations were made, one for compressive force, the other for traction. The results, figure 23 and 24, revealed that, this force, compressive or traction, had a negative influence in the cutting force, decreasing it more, the greater they were.

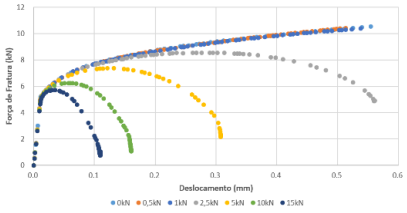

Figure 23- Traction normal force force-displacement curves;

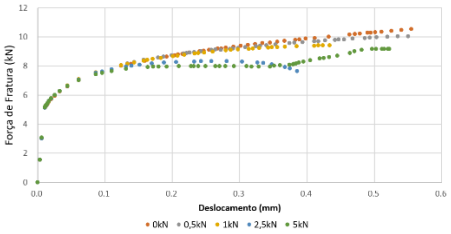

Figure 24- Compression normal force force-displacement curves;

The second set of predictions were about the tests done in this study. These simulations used the real geometry of the test piece used in the test.

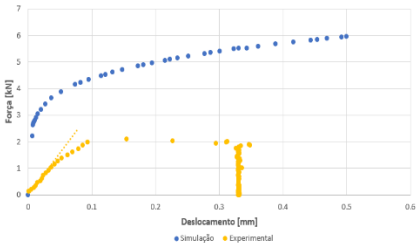

Figure 25- 0,5mm pure cut real and theoretical force-displacement curves;

Figure 25 shows the simulation and experimental result for the pure cut test of the 0,5mm test piece. This was a bad prediction, not truthfully predicting the cutting force. This difference is attributed to damage sustained by the test piece before the test.

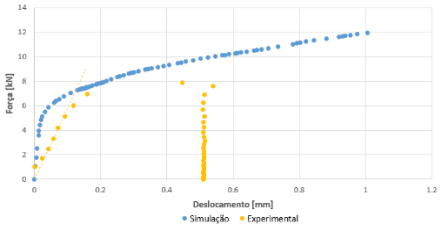

Figure 26-1mm pure cut real and theoretical force-displacement curves;

Figure 26 shows the simulation and experimental result for the pure cut test of the 1mm test piece. This simulation did a much better jog in predicting the cutting force, being very accurate at the moment of failure.

The previous test corroborated the result of the first prediction, that an

increase in resistant area has a positive influence in the cutting force.

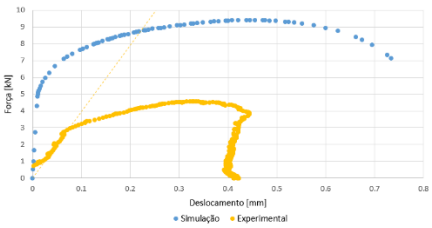

Figure 27- 1mm traction real and theoretical force-displacement curves;

Figure 27 shows the simulation and experimental result for the traction normal force test. This prediction wasn't very good, also, attributing the origin of this difference to the same reason of the 0,5mm test piece case.

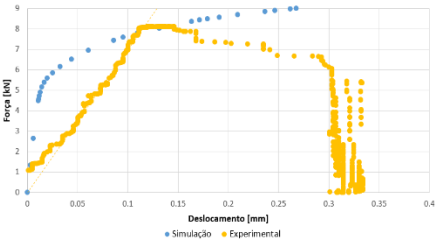

Figure 28- 1mm compression real and theoretical force-displacement curves;

Figure 28 shows the simulation and experimental result for the compressive normal force test. This prediction in much more accurate, also predicting with success the cutting force at the moment of fracture.

The three tests done with a 1mm test piece allows to check if the second prediction is correct, concluding the regarding the traction test the prediction was correct, the cutting force decreased, but for the compression the prediction wasn't correct, the cutting force being almost the same.

6. Conclusions

In the conclusion the main goal of this project was achieved successfully, resulting in the construction of a test machine able of simultaneously applying a cutting force in a test piece and putting the same test piece under different stress states, either compressive or traction.

Figure 29- Final test machine setup;

The secondary goal was only partially succeeded, resulting in an experimental procedure that allows a easy and fast way to quantify a materials mode II fracture toughness. However, some of the tests had unpredicted results, the origins of which weren't determined, due to the span of this study being too short.

7.References

Atkins, G., Ductile Fracture Mechanics, Key Engineering Materials Vol. 177-180, Trans Tech Publications, Switzerland, 2000

Gregório, Afonso J. V. L., Ensaios de impacto a elevadas velocidades de deformação, Instituto Superior Técnico, 2017

Silva C.M.A., "Influência da velocidade de deformação na tenacidade à fractura do chumbo-tecnicamente puro", MSc Tese, Universidade Técnica de Lisboa, outubro, 2007

Zhang, Y. & Chen, Z., On the Effect of Stress Triaxiality on Void Coalescence, Springer Science + Business Media B. V., 2007